

Hyperfine interaction with the ^{229}Th nucleus and its low-lying isomeric state

Robert A. Müller,^{1,2,*} Anna V. Maiorova,³ Stephan Fritzsche,^{4,5} Andrey V. Volotka,⁴ Randolph Beerwerth,^{4,5} Przemyslaw Glowacki,^{1,†} Johannes Thielking,¹ David-Marcel Meier,¹ Maksim Okhapkin,¹ Ekkehard Peik,¹ and Andrey Surzhykov^{1,2}

¹Physikalisch-Technische Bundesanstalt, D-38116 Braunschweig, Germany

²Technische Universität Braunschweig, D-38106 Braunschweig, Germany

³Center for Advanced Studies, Peter the Great St. Petersburg State Polytechnical University, Polytekhnicheskaya 29, 195251 St. Petersburg, Russia

⁴Helmholtz Institute Jena, D-07743 Jena, Germany

⁵Friedrich-Schiller-University Jena, D-07743 Jena, Germany



(Received 31 January 2018; published 20 August 2018)

The thorium nucleus with a mass number $A = 229$ has attracted much interest because its extremely low-lying first excited isomeric state at about 8 eV opens the possibility for the development of a nuclear clock. Both the energy of this state as well as the nuclear magnetic dipole and electric quadrupole moment of the ^{229m}Th isomer are subjects of intense research. The latter can be determined by investigating the hyperfine structure of thorium atoms or ions. Due to its electronic structure and the long lifetime of the nuclear isomeric state, Th^{2+} is especially suitable for such kinds of studies. In this Rapid Communication, we present a combined experimental and theoretical investigation of the hyperfine structure of the $^{229}\text{Th}^{2+}$ ion in the nuclear ground state, where a good agreement between theory and experiment is found. For the nuclear excited state we use our calculations in combination with recent measurements [J. Thielking *et al.*, *Nature (London)* **556**, 321 (2018)] to obtain the nuclear dipole moment of the isomeric state $\mu_{\text{iso}} = -0.35\mu_{\text{N}}$, which is in contradiction to the theoretically predicted value of $\mu_{\text{iso}} = -0.076\mu_{\text{N}}$ [A. M. Dykhne and E. V. Tkalya, *JETP Lett.* **67**, 251 (1998)].

DOI: [10.1103/PhysRevA.98.020503](https://doi.org/10.1103/PhysRevA.98.020503)

Introduction. While the energy levels of atomic nuclei are usually several keV, if not MeV, apart, ^{229}Th exhibits an extremely low-lying isomeric state ^{229m}Th with an excitation energy of only about 8 eV [1–3]. Since this energy can be reached by current laser systems and the nuclear isomer is very long lived, it has been proposed to build a nuclear clock based on the transition from the nuclear ground to the isomeric state [4]. The precision of this clock has been estimated to 10^{-19} s [5,6]. Therefore such a clock might be sensitive to temporal drifts of the quantum chromodynamics (QCD) coupling constant and the fine-structure constant. In fact, it was shown that the transition from the nuclear ground to the isomeric state could be orders of magnitude more sensitive to temporal variations of the fine-structure constant α than electronic transitions [7–10].

The experimental realization of a nuclear clock requires precise knowledge of the nuclear properties of both the nuclear ground and the first excited isomeric states. Most of the important quantities are not known to a high precision so far. The exact energy of the isomer, for example, remains to be determined. The currently accepted value of 7.8(5) eV has been obtained by a comparison of fluorescence lines in the keV regime from higher excited states of the ^{229}Th nucleus [11,12]. For the search for possible variations of the fundamental

constants, the moments of the nuclear ground and isomeric states [8,9] are of major importance. The moments of the ground-state nucleus have been extracted to a good precision by a combination of theory and experiment in Th^{3+} [13]. Moreover, recently, the first measurements of the moments of the nuclear isomer have been presented [7]. Since these were partially contradicting previous calculations [10,14], a theoretical explanation is still pending.

A well-established and precise method for determining nuclear moments is hyperfine spectroscopy: the measurement of the hyperfine splitting of electronic levels. The precise analysis of such experimental data requires both theoretical and experimental efforts. A theoretically challenging, but experimentally convenient, system for hyperfine spectroscopy of thorium is the charge state Th^{2+} , which resembles a two-valence electron system. The ionization threshold of this ion is well above the low-lying nuclear resonance [15] and the density of low energetic electronic levels is much smaller than in the case of Th^+ . Therefore the longevity of the nuclear isomer is increased, allowing for a better measurement statistic. However, except for the recent experiment [7], neither experimental nor theoretical values for the hyperfine structure in $^{229}\text{Th}^{2+}$ have been presented so far.

In this Rapid Communication, we present a comparative study of experimental values and theoretical calculations for the hyperfine splitting in both $^{229}\text{Th}^{2+}$ and $^{229m}\text{Th}^{2+}$. Our theoretical results are obtained using two different methods, a combination of configuration interaction and second-order many-body perturbation theory (CI+MBPT) and the

*robert.mueller@ptb.de

†Present address: Poznań University of Technology, 60-965 Poznań, Poland.

multiconfigurational Dirac-Fock approach (MCDF). The combination of these theories and experimental data allows for an evaluation of the $^{229\text{m}}\text{Th}^{2+}$ nuclear magnetic dipole and electric quadrupole moment, independent on previous determinations of these quantities [13]. This might support future investigations of possible variations of the fundamental constants.

Hyperfine structure of thorium ions. Hyperfine spectroscopy is the measurement of the splitting of atomic levels due to the coupling of the nuclear spin \vec{I} and the total angular momentum \vec{J} of the electronic state to the combined total angular momentum $\vec{F} = \vec{I} + \vec{J}$. The energy shift induced by that coupling can be calculated using first-order perturbation theory,

$$E_{M1} = \frac{1}{2}AC, \quad (1a)$$

$$E_{E2} = B \frac{\frac{3}{4}C(C+1) - I(I+1)J(J+1)}{2I(2I-1)J(2J-1)}, \quad (1b)$$

where $C = F(F+1) - J(J+1) - I(I+1)$. The subscript $M1$ refers to the energy shift due to the interaction of the electron shell with the magnetic dipole moment of the nucleus, while $E2$ is the corresponding shift due to the nuclear electric quadrupole moment. Usually, multipoles higher than the $E2$ interaction are negligible.

The hyperfine energies (1) scale with the so-called *hyperfine constants* A and B . For an electronic state characterized by its total angular momentum J and further quantum numbers γ , these constants are obtained as [16]

$$A = \frac{\mu_I}{I} \frac{1}{\sqrt{J(J+1)(2J+1)}} \langle \gamma J || \vec{T}^1 || \gamma J \rangle, \quad (2a)$$

$$B = 2Q \left[\frac{J(2J-1)}{(J+1)(2J+1)(2J+3)} \right]^{\frac{1}{2}} \langle \gamma J || \vec{T}^2 || \gamma J \rangle, \quad (2b)$$

It can be seen from the equation that A and B are proportional to the nuclear magnetic dipole and electric quadrupole moment μ_I and Q , respectively. The operators \vec{T}^k are the electronic parts of the hyperfine interaction. Relation (2) can be used to extract the nuclear moments from the hyperfine splitting of atomic lines.

Numerical calculations. The theoretical determination of the hyperfine constants A and B and hence the hyperfine structure of Th^{2+} requires the evaluation of the many-electron matrix elements of the hyperfine operator \vec{T}^k [cf. Eq. (2)]. We therefore need to obtain a precise representation of the many-electron wave functions of the corresponding states. In this Rapid Communication, we apply two different methods to approximate these wave functions.

The first technique we use to calculate the hyperfine constants in $^{229}\text{Th}^{2+}$ is the relativistic configuration interaction (CI). In CI, the ansatz for a many-electron wave function with a well-defined parity Π and total angular momentum J is a superposition of N so-called configuration state functions (CSFs) [16],

$$\Psi(\Pi, J) = \sum_{i=1}^N c_i \Phi_i(\Pi, J). \quad (3)$$

With these basis functions, the Hamiltonian matrix and its eigenvalues are calculated. The entries of the corresponding eigenvectors are the expansion coefficients c_i . This reduces the problem of constructing a complicated many-electron wave function to the diagonalization of a matrix.

The relativistic CI approach is well known for its performance to calculate the atomic structure of highly charged ions and is being actively developed to include QED corrections to atomic processes up to a very high precision [17–20]. For the determination of hyperfine constants in Th^{2+} , however, the correlation between core electrons and core-valence correlations are of major importance, which are typically neglected in CI for practical reasons. To overcome these problems, many-body perturbation theory (MBPT) can be used to account for core-core and core-valence correlations, while the dynamics of the valence electrons are still treated using CI. The results presented here were obtained using the package published in Ref. [21]. A detailed description of the method can be found, e.g., in Refs. [22–24].

Accurate wave functions can be constructed alternatively by applying the multiconfigurational Dirac-Fock (MCDF) method [16]. Here, the wave functions are also constructed as a superposition of CSFs. However, in contrast to CI, the CSFs are not fixed, but iteratively optimized to achieve self-consistency of the result. For our calculations we utilized the newest version of the GRASP2K package [25].

Experimental method. For the experimental investigation of the $^{229}\text{Th}^{2+}$ hyperfine structure we use ions stored in a radio-frequency linear Paul trap [26]. The ions are cooled to room temperature by collisions with a buffer gas (He) at 0.1 Pa pressure, which also depopulates metastable states via collisional quenching. To prepare a sample of Th^{2+} ions we first load 10^5 Th^+ ions into the trap via laser ablation and then generate doubly charged ions via photoionization. We reach a stable amount of 10^3 Th^{2+} ions, defined by an equilibrium of the ionization rate and losses due to chemical reactions with impurities in the buffer gas.

We study single-photon excitations at two different frequencies which can be addressed by external-cavity diode lasers (see Fig. 1). The levels $5f^2(J=4) : 15\,148\text{ cm}^{-1}$ and $5f^2(J=4) : 21\,784\text{ cm}^{-1}$ are excited from the electronic ground state $5f6d(J=4) : 0\text{ cm}^{-1}$ via laser radiation at 660.1 and 459.1 nm, respectively. Both upper levels possess a fluorescence decay channel in the visible spectrum that is detectable by photomultiplier tubes. In addition, the decay from $5f^2(J=4) : 21\,784\text{ cm}^{-1}$ is spectrally separated from the excitation, allowing for a detection free from the background of laser stray light.

Furthermore, our analysis includes hyperfine spectroscopy data from a previous experiment [7], which utilizes Doppler-free two-step laser excitation to achieve a higher resolution [27,28]. This experiment was conducted at the Maier-Leibnitz-Laboratorium at LMU Munich using a ^{233}U source, which produces thorium recoil ions via alpha decay with 2% of the ions being in the isomeric nuclear state. The selected transition in this case was from the $6d^2(J=2) : 63\text{ cm}^{-1}$ electronic state to $5f^2(J=0) : 29\,300\text{ cm}^{-1}$ via the $5f6d(J=1) : 20\,711\text{ cm}^{-1}$ intermediate state, using laser radiation at 484.3 nm for the first and 1164.3 nm for the second step.

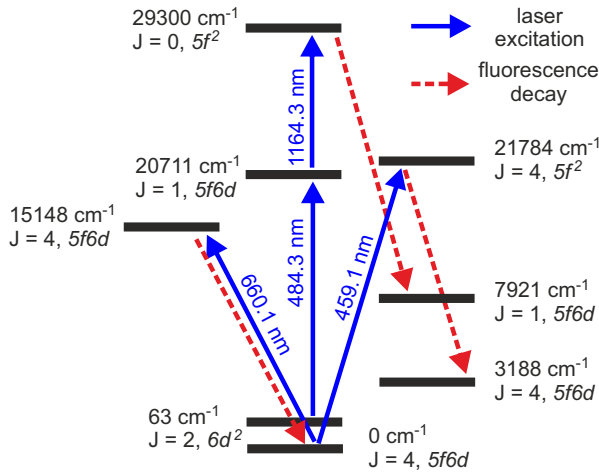


FIG. 1. Scheme of the investigated $^{229}\text{Th}^{2+}$ levels. The transitions and electronic configurations of Th^{2+} levels relevant to the experiment are depicted, labeled by their energy in cm^{-1} and the electronic angular momentum J . Laser excitation is shown with solid arrows and fluorescence detection with dashed arrows.

For detection, the fluorescence line from the decay of the $5f^2(J=0) : 29\,300 \text{ cm}^{-1}$ state to $5f6d(J=1) : 7921 \text{ cm}^{-1}$ was chosen.

Results and discussion. The hyperfine coefficients for $^{229}\text{Th}^{3+}$ were measured with high precision [29] and theoretical calculations of these coefficients have been presented in Ref. [13], including the extraction of the values $\mu_{\text{gr}} = 0.36\mu_{\text{N}}$ and $Q_{\text{gr}} = 3.11 \text{ eb}$ for the moments of the ground-state ^{229}Th nucleus. We used these moments to obtain the hyperfine constants for the ground and the first few excited states of $^{229}\text{Th}^{3+}$ using the MCDF method. We found these results to be in good agreement with previous calculations and thus the experimental values. Although triply charged thorium is a considerably simpler system, it resembles a very good test case for our calculations for Th^{2+} , because in both ions f and d orbitals are populated for the two lowest states, favoring strong core-valence correlation effects. The good agreement with the experiment thus gives us confidence that we are able to numerically control these correlations, also in the case of Th^{2+} .

While our calculations for triply charged thorium were an important benchmark, the complexity of the problem for doubly charged thorium is still considerably higher. The Th^{2+} ion has 45 levels in the desired energy range between 0 and $25\,000 \text{ cm}^{-1}$, ranging from three ($J^{\Pi} = 1^{-}$) to six ($J^{\Pi} = 2^{+}$ and $J^{\Pi} = 3^{-}$) for each pair of J and Π [cf. Eq. (3)]. Although only a few levels were addressed in the experiment, all of these levels need to be described to the same accuracy to obtain reliable theoretical results. Therefore the achievable accuracy of our calculations is worse than in other effective two-electron systems.

To obtain results for the level structure of the $^{229}\text{Th}^{2+}$ ion with the MCDF method, we first performed calculations, where the set of CSFs was constructed from a closed radon core allowing for double excitations of the two valence electrons. We added correlation layers until the energies of the calculated levels completely converged. These results were then used

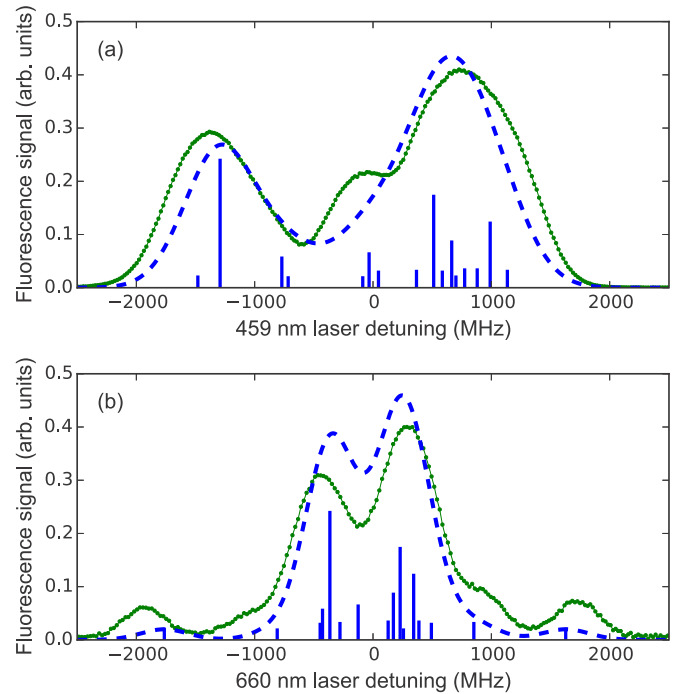


FIG. 2. Recorded $^{229}\text{Th}^{2+}$ hyperfine spectra. (a) Transition $5f6d(J=4) : 0 \text{ cm}^{-1}$ to $5f^2(J=4) : 21\,784 \text{ cm}^{-1}$, (b) transition $5f6d(J=4) : 0 \text{ cm}^{-1}$ to $5f^2(J=4) : 15\,148 \text{ cm}^{-1}$. Each subfigure shows the experimental data (connected dots) together with the positions of the individual resonances as predicted by MCDF calculations and the resulting theoretical spectrum (dashed line).

to perform calculations, where we subsequently added single excitations from the core up to the argon shell. After also allowing for core-valence excitations from the $6p$ and $5d$ orbitals we eventually achieved a very good convergence of the results. As it can be seen from Table I, our agreement with experimental excitation energies [30] is always better than 10%, except for the lowest $6d^2(J=2) : 63 \text{ cm}^{-1}$ state. The energy of this state is particularly difficult to obtain, because it is almost degenerate with the $5f6d(J=4) : 0 \text{ cm}^{-1}$ ground state. The accuracy of the CI+MBPT calculation is somewhat lower. The reason is strong correlations between two valence electrons and the outermost core shells. In order to increase the accuracy, one needs to go beyond the second-order MBPT and use CI+AO (CI+all-order) [31–33]. Our main goal here is to check that two very different methods give consistent results. For this purpose our CI+MBPT calculation is sufficient.

After we obtained the many-electron wave functions, we calculated the hyperfine coefficients for all states that were investigated experimentally. First, we used these results to analyze the spectra that have been obtained using the single-step excitation scheme (cf. Fig. 1). As seen in Fig. 2, the limited resolution of these spectra does not allow us to extract experimental values of the hyperfine constants for the electronic ground and the two $5f^2(J=4)$ states. Instead, we utilized the MCDF results for the A and B constants of these states (cf. Table I) to make a prediction for the positions of the individual resonances and the overall shape of the hyperfine spectrum. In Fig. 2 this prediction is shown alongside the

TABLE I. Magnetic dipole and electric quadrupole hyperfine constants A and B for the ground and four excited states of $^{229}\text{Th}^{2+}$. The theoretical results are obtained using CI+MBPT and the MCDF method. In lines two and four a comparison is drawn to experimental values presented in Ref. [7]. For the calculation, $\mu_{\text{gr}} = 0.36\mu_{\text{N}}$ and $Q_{\text{gr}} = 3.11|e|b$ have been used [13]. The experimental energies have been taken from Ref. [30].

Level		Energy (cm^{-1})			A (MHz)			B (MHz)		
Configuration	J^{Π}	CI+MBPT	MCDF	Expt. [30]	CI+MBPT	MCDF	Expt. [7]	CI+MBPT	MCDF	Expt. [7]
[Rn] + $5f6d$	4^{-}	0	0	0	64(17)	81(4)		3287(630)	3008(260)	
[Rn] + $6d^2$	2^{+}	2933	447	63	143(47)	162(8)	151(8)	68(23)	71(7)	73(27)
[Rn] + $5f^2$	4^{+}	23223	14891	15148	38(3)	72(3)		1221(390)	1910(200)	
[Rn] + $5f6d$	1^{-}	21193	22121	20711	109(36)	90(4)	88(5)	839(220)	689(110)	901(18)
[Rn] + $5f^2$	4^{+}	19946	21959	21784	8(36)	26(2)		65(21)	39(45)	

experimentally recorded spectra. While the positions of the main resonances match rather well, some discrepancies in the line intensities occur, especially for the $5f6d(J=4) : 0\text{ cm}^{-1}$ to $5f^2(J=4) : 21\,784\text{ cm}^{-1}$ transition. Moreover, the overall width of the calculated spectrum is slightly smaller than it was measured.

In contrast to the spectra recorded from the single-step excitation which were limited in resolution by Doppler broadening, the Doppler-free spectra, presented in Ref. [7], of the $6d^2(J=2) : 63\text{ cm}^{-1}$ and $5f6d(J=1) : 20\,711\text{ cm}^{-1}$ states allowed for a precise extraction of the hyperfine constants A and B . In Table I we show our numerical results alongside these experimentally extracted values. The theoretical uncertainty of the MCDF results is obtained from a convergence analysis with respect to the addition of correlation layers as well as the number of opened core shells. The uncertainty of the CI+MBPT results is determined by the neglected high-order MBPT terms. We estimated them from the size of the second-order MBPT and random phase approximation (RPA) corrections. We can see in Table I that the agreement between theory and experiment is very good for the magnetic hyperfine constant A . In the case of the electric quadrupole constant B , the agreement is slightly worse but still satisfying.

To obtain the values for the hyperfine constants A and B [cf. Eqs. (2)] shown in Table I, we used the nuclear moments of ^{229}Th from Ref. [13]. While these values for the ground-state nucleus are commonly accepted, the measured value of the nuclear dipole moment of the nuclear isomer $^{229\text{m}}\text{Th}$ [7] disagrees strongly with previous theoretical works [10,14]. As an example for a possible application of our calculations and to help to resolve this controversy, we calculated the atomic parts

A/μ_{iso} and B/Q_{iso} of the hyperfine constants in the doubly charged nuclear isomer $^{229\text{m}}\text{Th}^{2+}$, which has a nuclear spin of $I_{\text{iso}} = \frac{3}{2}$ in contrast to the nuclear ground state with $I_{\text{gr}} = \frac{5}{2}$. By combining these calculations with measurements for A and B , we can extract the nuclear moments of the nuclear isomer to a high precision. The results of these calculations are shown in Table II. In Ref. [7], μ_{iso} has been determined by measuring the ratio $\mu_{\text{iso}}/\mu_{\text{gr}}$ and using μ_{gr} from Ref. [13]. The obtained value of $\mu_{\text{iso}} = -0.37(6)\mu_{\text{N}}$ coincides with our consideration, which gives an average value of $\mu_{\text{iso}} - 0.35\mu_{\text{N}}$. Therefore, our calculations affirm the measurements and thus provide a stronger foundation for the obtained value of the magnetic dipole moment of the nuclear isomer $^{229\text{m}}\text{Th}$. An analog consideration for Q_{iso} shows a very good agreement between the value obtained using the CI+MBPT method and the experimental value of $Q_{\text{iso}} = 1.74(8)\text{ eb}$, while the result from the MCDF method is slightly above the measured result.

Concluding remarks. In summary, we aimed for a theoretical prediction of the hyperfine structure of doubly charged thorium with the nucleus being in the ground, and the first isomeric state. Therefore we employed two different approaches: (i) a combination of many-body perturbation theory and configuration interaction and (ii) the multiconfigurational Dirac-Fock method. We performed large-scale calculations for the hyperfine constants A and B in $^{229}\text{Th}^{2+}$. The results of these calculations were based on the nuclear moments [13] and reproduced the experimental data very well. That is, we provide an independent confirmation of the calculations presented by Safranova *et al.* in a system with a more complicated electronic structure and a different experimental setup. Finally, we also obtained the magnetic dipole moment of the nuclear isomer

TABLE II. Atomic part of the magnetic dipole hyperfine constant A/μ_{iso} for two excited states of $^{229\text{m}}\text{Th}^{2+}$. The results have been obtained using (a) the CI+MBPT and (b) the MCDF method. The experimental values presented in Ref. [7] are utilized to extract the magnetic dipole μ_{iso} and electric quadrupole Q_{iso} moment of the $^{229\text{m}}\text{Th}$ nuclear isomer.

Energy level		A/μ_{iso} (MHz/ μ_{N})			A (MHz)	μ_{iso} (μ_{N})		B/Q_{iso} (MHz/eb)		B (MHz)	Q_{iso} (eb)	
Configuration	J^{Π}	Energy (cm^{-1})	(a)	(b)	Expt. [7]	(a)	(b)	(a)	(b)	Expt. [7]	(a)	(b)
[Rn] + $6d^2$	2^{+}	63	660	749	-263(29)	-0.40	-0.35	22	23	53(65)		
[Rn] + $5f6d$	1^{-}	20711	506	419	-151(22)	-0.30	-0.36	270	222	498(15)	1.84	2.24

using measurements of the hyperfine constant A and calculations for the ratio A/μ_{iso} . Our result of $\mu_{\text{iso}} = -0.35\mu_N$ rules out a previous theoretical work that estimated the magnetic dipole moment to be $\mu_{\text{iso}} = -0.076\mu_N$. This discrepancy arose first in Ref. [7], where Ref. [13] has been used to obtain μ_{iso} . Our work complements these studies by providing an independent value for the nuclear magnetic dipole moment of $^{229\text{m}}\text{Th}$. Therefore our theory allows for a better understanding of the low-lying nuclear isomer. Combined with further theoretical and experimental investigations, our results will moreover help to use thorium as a testground for fundamental physics [8–10].

Acknowledgments. R.A.M. and A.V.M. would like to thank Mikhail Kozlov for his support and many helpful discussions. R.A.M. acknowledges support by the RS-APS. A.V.M. acknowledges support by the Ministry of Education and Science of the Russian Federation (Grant No. 3.1463.2017/4.6) and by RFBR (Grant No. 17-02-00216). We thank Lars von der Wense, Benedikt Seiferle, and Peter Thirof from LMU Munich for their contributions to joint experiments. We acknowledge financial support from the European Union's Horizon 2020 Research and Innovation Programme under Grant Agreement No. 664732 (nuClock) and from DFG through CRC 1227 (DQ-mat, project B04).

-
- [1] L. Kroger and C. Reich, *Nucl. Phys. A* **259**, 29 (1976).
 [2] C. W. Reich and R. G. Helmer, *Phys. Rev. Lett.* **64**, 271 (1990).
 [3] Z. O. Guimarães-Filho and O. Helene, *Phys. Rev. C* **71**, 044303 (2005).
 [4] E. Peik and M. Okhapkin, *C. R. Phys.* **16**, 516 (2015).
 [5] C. J. Campbell, A. G. Radnaev, A. Kuzmich, V. A. Dzuba, V. V. Flambaum, and A. Derevianko, *Phys. Rev. Lett.* **108**, 120802 (2012).
 [6] G. A. Kazakov, A. N. Litvinov, V. I. Romanenko, L. P. Yatsenko, A. V. Romanenko, M. Schreitl, G. Winkler, and T. Schumm, *New J. Phys.* **14**, 083019 (2012).
 [7] J. Thielking, M. V. Okhapkin, P. Głowacki, D. M. Meier, L. von der Wense, B. Seiferle, C. E. Düllmann, P. G. Thirolf, and E. Peik, *Nature (London)* **556**, 321 (2018).
 [8] V. V. Flambaum, *Phys. Rev. Lett.* **97**, 092502 (2006).
 [9] J. C. Berengut, V. A. Dzuba, V. V. Flambaum, and S. G. Porsev, *Phys. Rev. Lett.* **102**, 210801 (2009).
 [10] E. Litvinova, H. Feldmeier, J. Dobaczewski, and V. Flambaum, *Phys. Rev. C* **79**, 064303 (2009).
 [11] B. R. Beck, J. A. Becker, P. Beiersdorfer, G. V. Brown, K. J. Moody, J. B. Wilhelmy, F. S. Porter, C. A. Kilbourne, and R. L. Kelley, *Phys. Rev. Lett.* **98**, 142501 (2007).
 [12] E. V. Tkalya, C. Schneider, J. Jeet, and E. R. Hudson, *Phys. Rev. C* **92**, 054324 (2015).
 [13] M. S. Safronova, U. I. Safronova, A. G. Radnaev, C. J. Campbell, and A. Kuzmich, *Phys. Rev. A* **88**, 060501 (2013).
 [14] A. M. Dykhne and E. V. Tkalya, *JETP Lett.* **67**, 251 (1998).
 [15] L. von der Wense, B. Seiferle, M. Laatiaoui, J. B. Neumayr, H.-J. Maier, H.-F. Wirth, C. Mokry, J. Runke, K. Eberhardt, C. E. Düllmann, N. G. Trautmann, and P. G. Thirolf, *Nature (London)* **533**, 47 (2016).
 [16] I. P. Grant, *Relativistic Quantum Theory of Atoms and Molecules: Theory and Computation* (Springer, Berlin, 2007).
 [17] V. A. Yerokhin, A. N. Artemyev, V. M. Shabaev, M. M. Sysak, O. M. Zherebtsov, and G. Soff, *Phys. Rev. Lett.* **85**, 4699 (2000).
 [18] A. N. Artemyev, V. M. Shabaev, I. I. Tupitsyn, G. Plunien, and V. A. Yerokhin, *Phys. Rev. Lett.* **98**, 173004 (2007).
 [19] N. S. Oreshkina, D. A. Glazov, A. V. Volotka, V. M. Shabaev, I. I. Tupitsyn, and G. Plunien, *Phys. Lett. A* **372**, 675 (2008).
 [20] V. A. Yerokhin and A. Surzhykov, *Phys. Rev. A* **86**, 042507 (2012).
 [21] M. Kozlov, S. Porsev, M. Safronova, and I. Tupitsyn, *Comput. Phys. Commun.* **195**, 199 (2015).
 [22] V. A. Dzuba, V. V. Flambaum, and M. G. Kozlov, *Phys. Rev. A* **54**, 3948 (1996).
 [23] V. A. Dzuba, *Phys. Rev. A* **71**, 032512 (2005).
 [24] V. A. Dzuba and V. V. Flambaum, *Phys. Rev. A* **75**, 052504 (2007).
 [25] P. Jönsson, G. Gaigalas, J. Bieroń, C. F. Fischer, and I. Grant, *Comput. Phys. Commun.* **184**, 2197 (2013).
 [26] O. A. Herrera-Sancho, M. V. Okhapkin, K. Zimmermann, C. Tamm, E. Peik, A. V. Taichenachev, V. I. Yudin, and P. Głowacki, *Phys. Rev. A* **85**, 033402 (2012).
 [27] J. E. Bjorkholm and P. F. Liao, *Phys. Rev. A* **14**, 751 (1976).
 [28] W. Kälber, J. Rink, K. Bekk, W. Faubel, S. Göring, G. Meisel, H. Rebel, and R. C. Thompson, *Z. Phys. A: At. Nucl.* **334**, 103 (1989).
 [29] C. J. Campbell, A. G. Radnaev, and A. Kuzmich, *Phys. Rev. Lett.* **106**, 223001 (2011).
 [30] A. Kramida, Yu. Ralchenko, J. Reader, and NIST ASD Team, (2015) published: NIST Atomic Spectra Database (ver. 5.3) (online), available at <http://physics.nist.gov/asd> (25 September 2017), National Institute of Standards and Technology, Gaithersburg, MD.
 [31] M. G. Kozlov, *Int. J. Quantum Chem.* **100**, 336 (2004).
 [32] M. S. Safronova, M. G. Kozlov, W. R. Johnson, and D. Jiang, *Phys. Rev. A* **80**, 012516 (2009).
 [33] M. V. Okhapkin, D. M. Meier, E. Peik, M. S. Safronova, M. G. Kozlov, and S. G. Porsev, *Phys. Rev. A* **92**, 020503 (2015).